IEEE Access
Multidisciplinary | Rapid Review | Open Access Journal

Received November 5, 2019, accepted November 18, 2019, date of publication November 25, 2019,
date of current version December 9, 2019.

Digital Object Identifier 10.1109/ACCESS.2019.2955471

Theoretical and Experimental Investigation of an All-Fiber Waveguide Coupled Surface Plasmon Resonance Sensor With Au–ZnO–Au Sandwich Structure

JINYING MA, KUN LIU, JUNFENG JIANG, TIANHUA XU, SHUANG WANG, PENGXIANG CHANG, ZHAO ZHANG, JIAHANG ZHANG, AND TIEGEN LIU

School of Precision Instruments and Optoelectronics Engineering, Tianjin University, Tianjin 300072, China
Key Laboratory of Optoelectronics Information Technology, Ministry of Education, Tianjin University, Tianjin 300072, China
Tianjin Optical Fiber Sensing Engineering Center, Institute of Optical Fiber Sensing, Tianjin University, Tianjin 300072, China

Corresponding authors: Kun Liu (beiyangkl@tju.edu.cn) and Junfeng Jiang (jiangjfjxu@tju.edu.cn)

This work was supported in part by the National Natural Science Foundation of China under Grant 61922061, Grant 61775161, and Grant 61775011, and in part by the National Instrument Program under Grant 2013YQ030915.

ABSTRACT In this paper, we proposed an all-fiber waveguide coupled surface Plasmon resonance (SPR) sensor which was designed and fabricated with Au-ZnO-Au sandwich multi-layer structure. Based on the transfer matrix method (TMM), the theoretical modeling of the proposed sensor structure was investigated. The influence of the layer thickness on the transmission spectrum of the sensor was studied numerically, in order to optimize each layer thickness, leading to sensitivity enhancement in the infrared spectral range. Meanwhile, an experimental testbed for the refractive index measurement was implemented based on the proposed all-fiber waveguide coupled SPR sensor. Using this waveguide coupled SPR sensor, the refractive index sensing was realized with a sensitivity enhancement of 7%—131% compared with conventional SPR sensors.

INDEX TERMS Surface plasmon resonance, optical fiber, waveguide coupled, sensitivity, refractive index sensing.

I. INTRODUCTION

The surface Plasmon resonance (SPR) technique is gradually becoming a more popular focus of research [1]–[5], since the SPR phenomenon was observed experimentally by Wood at the beginning of the twentieth century [6]. The SPR technique has been widely applied in many areas such as biology, physics, chemistry and many other fields [7]. Jorgenson for the first time reported an SPR sensor based on a multimode optical fiber in 1993, leading to a new research direction [8]. The fiber-based SPR sensors are very sensitive to the refractive index [9], temperature [10] and other factors. Together with the advantages of fiber such as smart size, high response speed, remote detection and easy coupling with microfluidics, the fiber-based SPR sensor shows tremendous prospects for the development of biological and gaseous sensing research.

As one of the most important research areas in optical fiber sensing technologies, fiber-based SPR sensors focus on improving the limit detection by using various structures [11]. The waveguide coupled SPR sensor is a relatively novel and effective structure developed in recent years [12], [13]. By including a slab of dielectric material between two metal layers, the waveguide coupled SPR sensor not only prevents the interaction of the two metals but also acts as a waveguide medium between them [14]. This will lead to a much better performance due to sharper resonance dip. The waveguide coupled SPR sensor was realized by Toyama et al., using the angle modulation based on a prism configuration [15], and the limit of detection of 6×10^{-6} RIU as 3 times the refractive index sensing resolution of the sensor was then obtained by Song et al., in 2013 [16]. Currently, waveguide coupled SPR sensors have only been used for

The associate editor coordinating the review of this manuscript and approving it for publication was Sukhdev Roy.

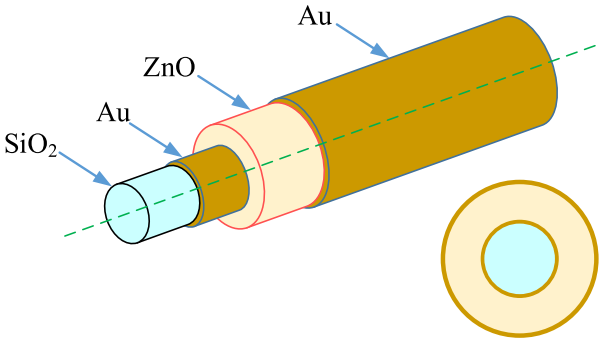

FIGURE 1. The schematic diagram of all-fiber waveguide coupled SPR sensor with Au-ZnO-Au sandwich structure.

laboratory-based research. But when it is applied to the antibody and antigen on-line measurement, the prism-based waveguide coupled SPR sensor appears too complex for obtaining stable and accurate results. However, a fiber-based waveguide coupled SPR sensor has the potential to solve this problem. To the best of our knowledge, no systematic investigation has been performed until now.

In this paper, an all-fiber waveguide coupled SPR sensor was developed and investigated both theoretically and experimentally. This SPR sensor was designed and fabricated with Au-ZnO-Au sandwich structure. The theoretical model was investigated using the transfer matrix method, in order to optimize the layer thickness for the SPR sensor. Based on this all-fiber waveguide coupled SPR sensor, the measurement of the refractive index was realized with a high sensitivity (2198-4732 nm/RIU). Finally, experimental results were discussed and compared with a conventional SPR sensor in terms of sensitivity.

II. THEORETICAL SIMULATION

A. BASIC MODEL

The all-fiber waveguide coupled SPR sensor was designed as shown in Fig. 1. The SiO_2 based optical fiber core was covered by a sandwich type multi-layer structure of Au-ZnO-Au. The inner and outer layers of gold are both thin, while the dielectric layer of zinc oxide is thick enough to support the waveguide modes [17]. Unlike the traditional fiber SPR sensor with a dip only in the p-polarized light [10], the waveguide coupled fiber SPR sensor covered with Au-ZnO-Au layers will cause sharp dips in both the p-polarized and s-polarized lights due to the interference in the dielectric layer [18].

The transfer matrix method (TMM) was applied to analyze the reflection and transmission characteristics of the waveguide coupled fiber SPR sensor, covered by Au-ZnO-Au structure [12]. TMM treats the reflection and transmission at the interface of two media as one matrix. The one-dimensional cross section of the sensor shown in Fig. 1 can be regarded as a stack of the multi-layer structures with geometrical thickness of d_k and refractive indices of n_k for the k^{th} film layer. The electric and magnetic field amplitudes (E and H) can be expressed using the characteristic matrix equation as [12]

$$\begin{bmatrix} E_1 \\ H_1 \end{bmatrix} = M \begin{bmatrix} E_N \\ H_N \end{bmatrix} \tag{1}$$

where E_1 and H_1 are the components of the electric and magnetic fields at the boundary of the first layer, E_N and H_N are the components of the electric and magnetic fields of the Nth layer, and M denotes the transfer matrix of the multi-layer structure. The transfer matrix M can be described as the linear product of the transfer matrix M_k for the boundary between the kth and $(k+1)$th layer as

$$M = \prod_{k=1}^{N-1} M_k = \begin{bmatrix} M_{11} & M_{12} \\ M_{21} & M_{22} \end{bmatrix} \tag{2}$$

The transfer matrix M_k can be written as

$$M_k = \begin{bmatrix} \cos\phi_k & -i\sin\phi_k / \eta_k \\ -i\eta_k \sin\phi_k & \cos\phi_k \end{bmatrix} \tag{3}$$

where $\phi_k = \left(2\pi/\lambda\right)(n_k \cos\theta_k)\, d_k$ represents the phase factor of the kth layer, λ is the optical wavelength, θ_k is the angle of the incidence for the kth layer, and η_k denotes the optical admittance for the kth layer. The reflectance R can be calculated as [19]

$$R = |r|^2 = \left| \frac{(M_{11} + M_{12}\eta_N)\eta_1 - (M_{21} + M_{22}\eta_N)}{(M_{11} + M_{12}\eta_N)\eta_1 + (M_{21} + M_{22}\eta_N)} \right|^2 \tag{4}$$

The normalized transmitted power, P_{trans}, in the fiber SPR sensor will be then expressed as

$$P_{trans} = \frac{\int_{\theta_{cr}}^{\pi/2} R^{N_{ref}(\theta)} \frac{n_1^2 \sin\theta\cos\theta}{\left(1-n_1^2\cos^2\theta\right)^2} d\theta}{\int_{\theta_{cr}}^{\pi/2} \frac{n_1^2 \sin\theta\cos\theta}{\left(1-n_1^2\cos^2\theta\right)^2} d\theta} \tag{5}$$

where

$$N_{ref}(\theta) = \frac{L}{D_c \tan\theta} \tag{6}$$

and

$$\theta_{cr} = \sin^{-1}\left(\frac{n_{cl}}{n_1}\right) \tag{7}$$

In Eq. (6) N_{ref} represents the total number of reflections in the sensing region, while L and D_C represent the length of the exposed sensing region and the diameter of the fiber core, respectively. In Eq. (7) θ_{cr} is the critical angle of the fiber, whereas n_{cl} is the refractive index of the fiber cladding.

B. INFLUENCE OF LAYER THICKNESS

Based on the model developed in Section II. A, the normalized transmission spectrum of the all-fiber waveguide coupled SPR sensor can be calculated accordingly. The exposed sensing length and the fiber core diameter were set as $L = 10$ mm and $D_c = 600$ mm respectively. The refractive index n_k of each film layer and fiber cladding were calculated according to the Drude model [18], [19].

When the thicknesses of the outer gold and zinc oxide layer were set as 16 nm and 300 nm respectively, the normalized

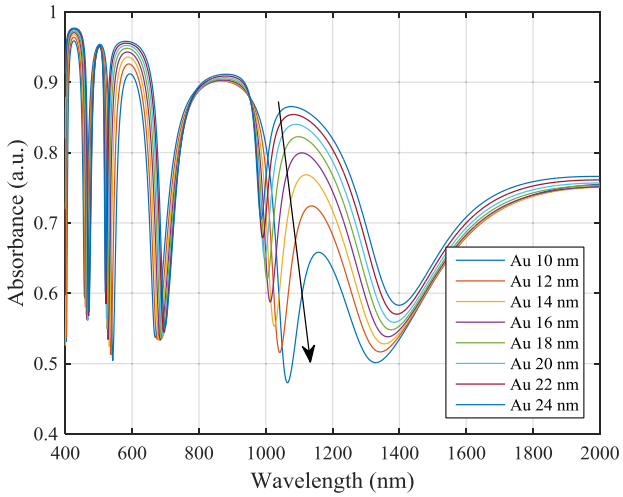

FIGURE 2. Normalized transmission spectrum for different thicknesses of the inner gold layer with the thickness of the outer gold layer set as 16 nm and the thickness of the zinc oxide layer set as 300 nm.

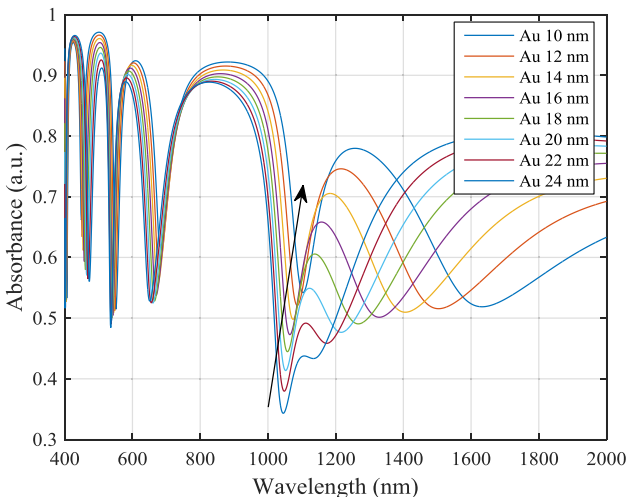

FIGURE 3. Normalized transmission spectrum for different thicknesses of the outer gold layer with the thickness of the inner gold layer set as 10 nm and the thickness of the zinc oxide layer set as 300 nm.

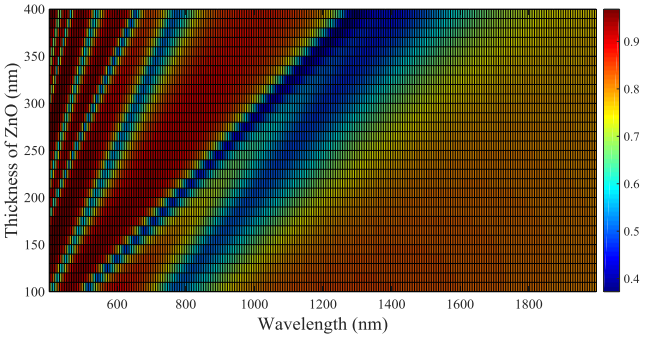

FIGURE 4. Normalized transmission spectra for different thicknesses of the zinc oxide layer with the thickness of the inner and outer gold layer set as 10 nm and 20 nm respectively.

transmission spectra corresponding to different thicknesses of the inner gold layer were computed and shown in Fig. 2, where the deionized water is employed as the test medium with a refractive index of 1.333. It can be seen that there are many absorption valleys in the transmission spectra for the all-fiber waveguide coupled SPR sensor. As the thickness of the inner gold layer increases, the depths of the valleys get decreased. This is because that there is not enough optical energy coupled into the test medium through the zinc oxide and outer gold layer, if the thickness of the inner gold layer is too large. On the other hand, the thickness of the inner gold layer cannot be too small, otherwise the SPR phenomenon will disappear. According to Fig. 2, we obtained the optimal thickness of the inner gold layer as 10 nm.

When the thicknesses of the inner gold and the zinc oxide layer were set as 10 nm and 300 nm respectively, the normalized transmission spectra corresponding to different thicknesses of the outer gold layer were calculated and described as shown in Fig. 3, with deionized water as the detected media with a refractive index of 1.333. Similar to Fig. 2, there are also many absorption valleys in each spectrum. With the increase of the thickness of the inner gold layer, the depth of the valleys will also increase due to the enhancement of the SPR phenomenon. But when the thickness of the outer gold layer exceeds 20 nm, there will be two valleys overlapped with each other. This leads to the difficulty in the demodulation. Therefore, we chose the optimal thickness of the inner gold layer as 20 nm.

When the thicknesses of the inner and outer gold layer were set as 10 nm and 20 nm respectively, the normalized transmission spectra corresponding to different thicknesses of the zinc oxide layer were simulated and illustrated in Fig. 4. The deionized water with a refractive index of 1.333 is again the test medium. When the thickness of the zinc oxide layer increases, the number of absorption valleys will also increase. When the thickness is about 100 nm, there will be three modes excited. However, when the thickness is larger than 350 nm, there will be seven modes excited. With the increase of the zinc oxide layer thickness, the red shift phenomenon will occur for all modes with different rates, and the absorption will enhance with spectral spreading. So when the thickness is over 350 nm, the two absorption alleys in infrared spectral range will overlap with each other and cannot be demodulated separately. To obtain a better spectrum for an easy demodulation, we chose the thickness of the zinc oxide layer to be 280 nm.

C. THE SENSITIVITY OF FIBER WAVEGUIDE COUPLED SPR SENSOR

According to the discussion above, we set the thicknesses of the inner gold layer, the zinc oxide layer and the outer gold layer as 10 nm, 280 nm and 20 nm respectively. When the refractive index of the test medium was changed from 1.333 to 1.403 with an interval of 0.01, the normalized transmission spectra were analyzed, as shown in Fig. 5. It is clearly seen that five modes are excited in the spectra. Three modes shifted with the change of the refractive index were

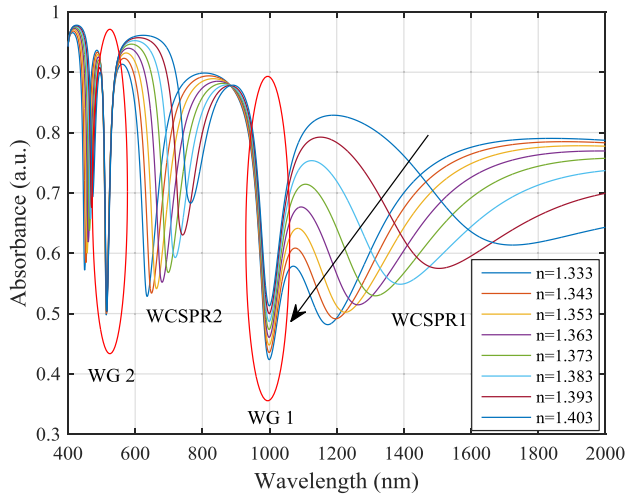

FIGURE 5. Normalized transmission spectra for different refractive indices of the test medium with the thicknesses of the inner gold layer, the zinc oxide layer and the outer gold layer set as 10 nm, 280 nm and 20 nm respectively.

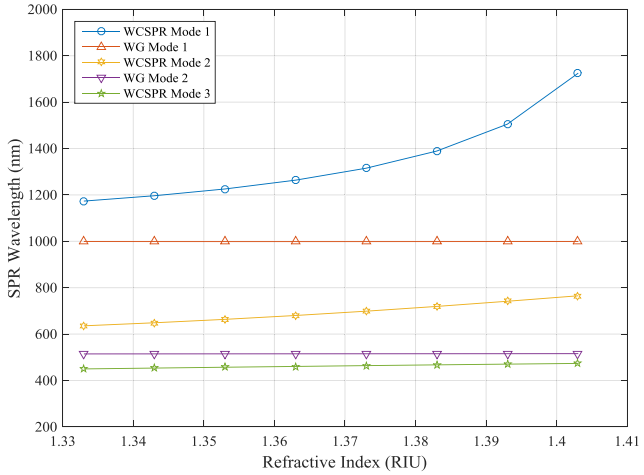

FIGURE 6. The relationship between the absorption wavelength and the refractive index of the test medium for the fiber waveguide coupled SPR sensor.

caused by the SPR phenomenon, and thus they were named waveguide coupled SPR (WCSPR) modes. Meanwhile, two modes, which do not shift with the change of the refractive index, were induced by the zinc oxide as a dielectric medium without any coupling with the test medium. So the two modes were named waveguide (WG) modes. The transmission spectrum is the combination of both phenomena, and there will be an SPR mode between any two waveguide modes. So this type of sensor was called as the waveguide coupled SPR sensor.

The absorption wavelength of each valley in Fig. 5 can be obtained by an extreme value search algorithm. The relationship between the absorption wavelength and the refractive index of the test medium for the fiber waveguide coupled SPR sensor was shown in Fig. 6. The wavelengths of the two WG modes keep nearly constant with the change of the refractive

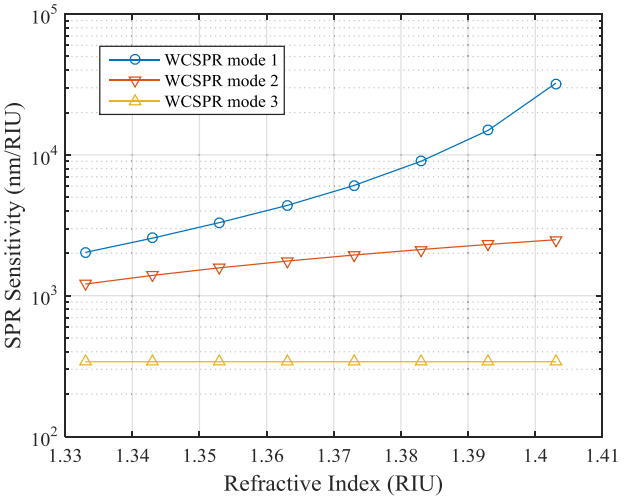

FIGURE 7. The theoretical sensitivity for WCSPR mode of the fiber waveguide coupled SPR sensor.

index, while the wavelengths of the three WCSPR modes will increase with the increment of the refractive index. We can also theoretically calculate the sensitivity as the wavelength shift of per refractive index unit (RIU) for each WCSPR mode as shown in Fig. 7, according to the sensitivity definition in references [20], [21]. When the sensor was used for detecting the test medium with a relatively higher refractive index, the sensitivity will increase dramatically. And for the WCSPR modes with long absorption wavelengths, the sensitivity will be even higher. Compared to the WCSPR modes in visible spectral range, the WCSPR mode in infrared spectral range can enhance the sensitivity by one order of magnitude or more for the test media with refractive index around 1.4 RIU. Even for the WCSPR mode in the visible spectral range, the sensitivity is also significantly higher than the conventional fiber SPR sensor with the gold layer only.

III. EXPERIMENTAL RESULTS AND DISCUSSION

Based on the theoretical simulation, the all-fiber waveguide coupled SPR sensor was fabricated on a plastic clad silica multimode optical fiber from Scitlion Technology with the numerical aperture of 0.37 and the core diameter of 600 μm respectively. In the center of the fiber, there is a 10 mm unclad section, which was cleaned by acetone and ethanol successively in the ultrasonic cleaner. The unclad section was coated by the sandwich multi-layer structure of 10 nm Au (inner), 135 nm ZnO waveguide (middle) and 20 nm Au (outer), using the RF magnetron sputtering method at a room temperature of 25 °C. The working pressure was 1 Pa (7.5 mTorr) in pure Ar atmosphere. The RF power was set to 60 W for the ceramic ZnO target and 33 W for the metallic Au target. All targets were 2 inches in diameter and 99.999% pure, purchased from ZhongNuo Advanced Material. The thickness of each layer was adjusted from the deposition rate and experimentally determined under the same conditions. According to the experimental calibration of the film thickness monitor, the deposition rates of Au and ZnO are

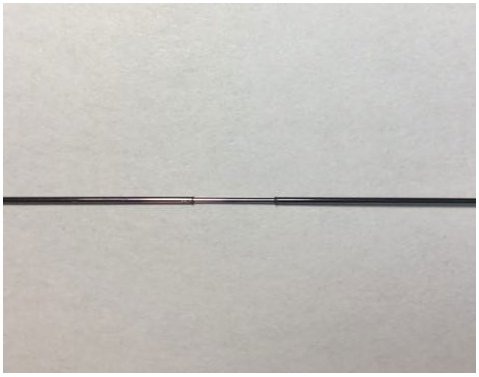

(a) The picture of the waveguide coupled SPR sensor

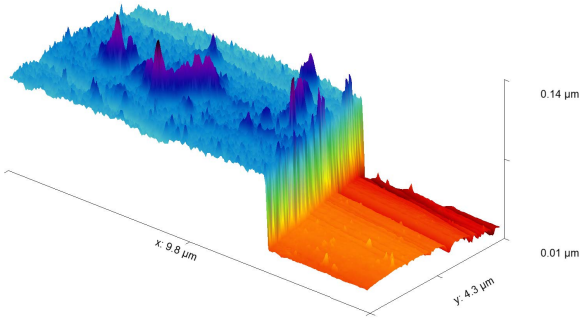

(b) The partial AFM photograph of the waveguide coupled SPR sensor

FIGURE 8. The waveguide coupled SPR sensor setup and partial AFM photograph.

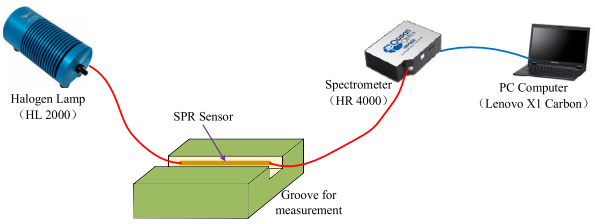

FIGURE 9. The experimental system of the waveguide coupled SPR refractive index sensor.

20.98 nm/min and 3.94 nm/min respectively. The WCSPR sensor setup and its partial atomic force microscopy (AFM) photograph are shown in Fig. 8. The films were well coated on the core of the optical fiber. For the Au-ZnO-Au sandwich multi-layer film with the thickness of 165 nm in whole, the roughness of the film is only 6.035 nm, while the roughness of the optical fiber core is 3.887 nm.

To verify the effectiveness of the waveguide coupled SPR sensor, an alcoholic solution refractive index sensing system was implemented. As shown in Fig. 9, the system consists of four parts, a tungsten halogen light source (model HL 2000, Ocean Optics), a waveguide coupled SPR sensor, a spectrophotometer (model HR 4000, Ocean Optics) and a computer. The light from the polychromatic source (a tungsten halogen light source with spectra of 360-2000 nm and input power of 100 W) was injected into the multimode fiber and passed through the waveguide coupled SPR sensor. The sensor was laid in the groove for easy immersion in the alcoholic solution. The transmitted light from the sensor was

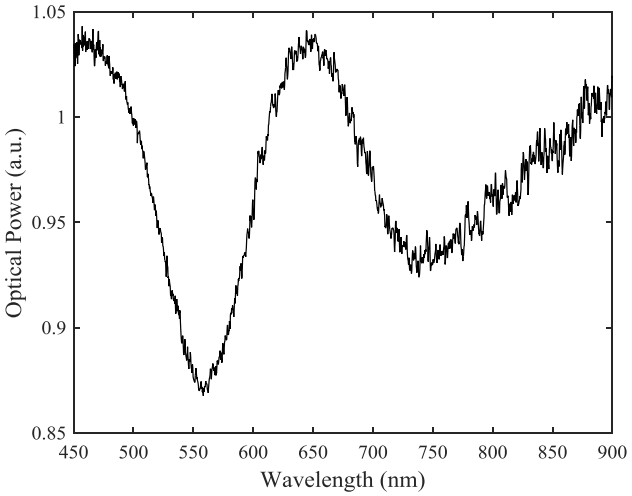

FIGURE 10. The transmission spectrum for deionized water with a refractive index of 1.333.

measured by the spectrophotometer with a detection range of 200-1100 nm and a resolution of 20 pm. Finally the light signals were stored and analyzed in the computer.

Based on the experimental system shown in Fig. 9, the transmission spectrum of the waveguide coupled SPR sensor can be obtained considering the influence of a tungsten halogen light source. The tungsten halogen light source can be directly collected without the sensor. The true transmission spectrum of the waveguide coupled SPR sensor can be calculated by separating the sensing signal spectrum from the source spectrum after the normalization of both spectra. Taking the deionized water with a refractive index of 1.333 as an example, the true transmission spectrum was detected and shown in Fig. 10. According to the wavelength range of light source and spectrophotometer, the spectrum collection range was from 360 nm to 1100 nm. In order to enhance the sensitivity of the collected spectrum, the integration time of the spectrophotometer was increased, leading to an effective spectrum collection wavelength range of 450-900 nm for the whole system. According to Fig. 10, there are two absorption valleys. The dip on the left side is the WG mode, while the dip on the right side is the WCSPR mode. The power weighing method can be used for extracting the wavelength for each valley after filtering and de-noising algorithm. For the dielectric layer of ZnO, the thickness should be $\lambda/2n$ or greater, where λ is the excitation wavelength and n is the refractive index of the dielectric layer [17]. For the 135 nm thick zinc oxide, the wavelength of the WG mode should be 549 nm, close to the true value of 558 nm in Fig. 10. Additionally, the absorbance of the WG mode is more than that of the WCSPR mode in Fig. 10, which is in accordance with the simulation results in Fig. 5.

The refractive index of the alcoholic solution can be changed by varying the concentration of the alcohol. The actual refractive index of the alcoholic solution was detected by Abbe refractometer. Meanwhile, the transmission spectrum of the sensor can be obtained through the experimental

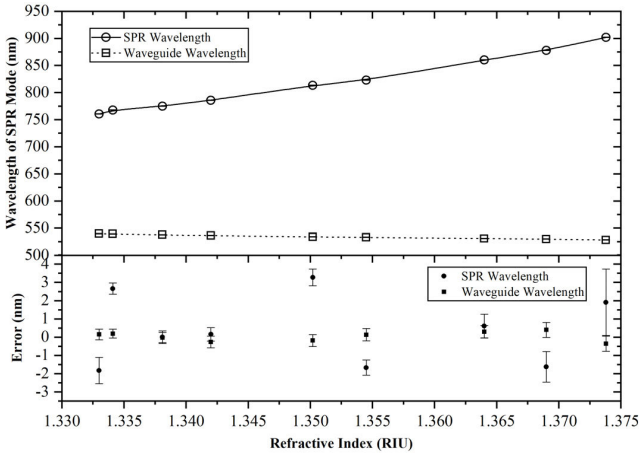

FIGURE 11. The relationship between the refractive index and the central wavelength.

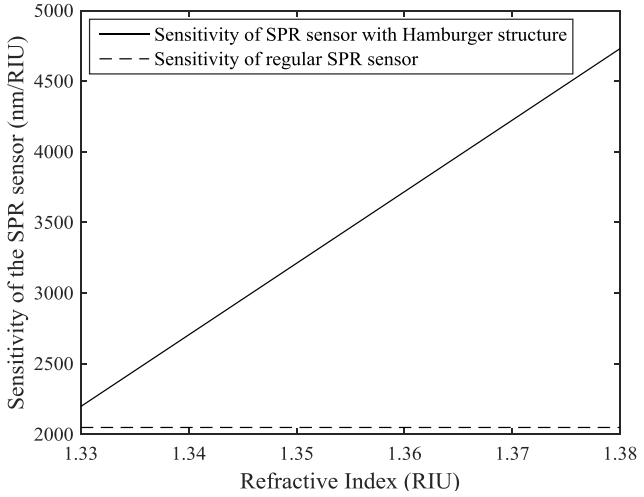

FIGURE 12. The sensitivity comparison between the waveguide coupled and conventional SPR sensors.

system and the wavelength for each valley can be calculated corresponding to alcoholic solution with different refractive index. The relationship between the refractive index and the central wavelength for each valley is shown in Fig. 11, with error bars for each refractive index respectively. The 100 sets of transmission spectrum corresponding to each refractive index were acquired for the WCSPR mode and the WG mode respectively. The error of the wavelength for the WCSPR mode is between -2.543 nm and 3.731 nm, while the error of the wavelength for the WG mode is between -0.779 nm and 0.801 nm. It can be seen form Fig. 11 that the wavelengths of the WCSPR mode shift with the change of the refractive index, and the relationship between them is $\lambda = 25334\text{RIU}^2 - 65190\text{RIU} + 42646$ with a fitting correlation coefficient of 0.9991. Meanwhile, the wavelength for WG mode keep nearly constant even when the refractive index changes.

The sensitivity of the all-fiber waveguide coupled SPR sensor was also compared to the conventional SPR sensor. The sensitivity can be calculated by $\delta\lambda_{res}/\delta n_s$, where δn_s and $\delta\lambda_{res}$ represent the variations in the refractive index of the medium and the corresponding resonance wavelength shift, respectively [22]. The sensitivity of the waveguide coupled SPR sensor can be obtained from the fitting relationship equation mentioned above by calculating the derivative values corresponding to different refractive index of the alcoholic solution, and this sensitivity is proportional to the refractive index value as $d\lambda/d\text{RIU} = 50668\text{RIU} - 65190$. The sensitivity of the conventional SPR sensor is 2048 nm/RIU as an constant from our previously work [23], while the sensitivity of the conventional SPR sensor is 2000 nm/RIU as an constant from Li's work [24]. The sensitivities of both SPR sensors were shown in Fig. 12. It is depicted that the sensitivity of the waveguide coupled SPR sensor can be enhanced by 7%—131% compared to the conventional SPR sensor of our previously work, according to the ratio of the sensitivities for the two type sensors corresponding to the same refractive index value. Restrained by the operation wavelength range in the experimental system, we can only measure the SPR in visible spectral range. If thicker dielectric layers of zinc oxide were coated and the SPR mode in the infrared spectral range was excited, the sensitivity will be enhanced even further.

IV. CONCLUSION

In this paper, an all-fiber waveguide coupled SPR sensor scheme was proposed, designed and fabricated, with an Au-ZnO-Au sandwich multi-layer structure. The theoretical model of the waveguide coupled SPR sensor was investigated. By analyzing the transmission spectrum of the sensor, the influence of the thickness for each layer was studied, and an optimal thickness of inner-Au (10 nm)/ZnO waveguide (280 nm)/outer-Au (20 nm) was found. The sensitivity enhancement of the sensor in infrared spectral range was also investigated. According to the theoretical simulation, an all-fiber waveguide coupled SPR sensor was realized and fabricated. The refractive index sensing system was implemented using the waveguide coupled SPR sensor. Compared to the conventional SPR sensor, the sensitivity can be enhanced by 7%—131% in visible spectral range. If a thicker ZnO layer is coated and the SPR mode in the infrared spectral range is excited, the sensitivity can be further enhanced. This proposed sensor can be applied for biological and gaseous molecules sensing with high precision.

ACKNOWLEDGMENT

The authors also would like thank Mr. B. Seeberger for grammatical corrections.

REFERENCES

[1] S. Shukla, N. K. Sharma, and V. Sajal, "Sensitivity enhancement of a surface plasmon resonance based fiber optic sensor using ZnO thin film: A theoretical study," *Sens. Actuators B, Chem.*, vol. 206, no. 23, pp. 463–470, Jan. 2015.

[2] R. Tabassum and B. D. Gupta, "Performance analysis of bimetallic layer with zinc oxide for SPR-based fiber optic sensor," *J. Lightw. Technol.*, vol. 33, no. 22, pp. 4565–4571, Nov. 15, 2015.

[3] P. Singh, "SPR biosensors: Historical perspectives and current challenges," *Sens. Actuators B, Chem.*, vol. 229, pp. 110–130, Jun. 2016.
[4] C. Liu, W. Su, X. Lu, F. Wang, T. Sun, and P. K. Chu, "Symmetrical dual D-shape photonic crystal fibers for surface plasmon resonance sensing," *Opt. Express*, vol. 26, no. 7, pp. 9039–9049, Apr. 2018.
[5] J.-Y. Jing, Q. Wang, W.-M. Zhao, and B.-T. Wang, "Long-range surface plasmon resonance and its sensing applications: A review," *Opt. Lasers Eng.*, vol. 112, no. SI, pp. 103–118, Jan. 2019.
[6] R. W. Wood, "On a remarkable case of uneven distribution of light in a diffraction grating spectrum," *Proc. Phys. Soc. London*, vol. 18, no. 1, pp. 396–402, 1902.
[7] Y. Wu, H. P. Ho, C. L. Wong, S. K. Kong, and C. Lin, "Surface plasmon resonance biosensor incorporated in a michelson interferometer withenhanced sensitivity," *IEEE Sensors J.*, vol. 7, no. 1, pp. 70–73, Jan. 2007.
[8] R. C. Jorgenson, "Surface Plasmon resonance based bulk optic and fiber optic sensors," Ph.D. dissertation, Dept. Electron. Elect., Univ. Washington, Washington, DC, USA, 1993.
[9] J. Zeng, D. K. Liang, Z. W. Zeng, and Y. Du, "Study on measurement of liquid refractive index by analyzing SPR spectrum character," (in Chinese), *Spectrosc. Spect. Anal.*, vol. 26, no. 4, pp. 723–727, Apr. 2006.
[10] T. Wang, T. Liu, K. Liu, J. Jiang, M. Xue, and Y. X. Meng, "An EMD-based filtering algorithm for the fiber-optic SPR sensor," *IEEE Photon. J.*, vol. 8, no. 3, Jun. 2016, Art. no. 6803008.
[11] C. Caucheteur, T. Guo, and J. Albert, "Review of plasmonic fiber optic biochemical sensors: Improving the limit of detection," *Anal. Bioanal. Chem.*, vol. 407, no. 14, pp. 3883–3897, May 2015.
[12] K. Tiwari, S. C. Sharma, and N. Hozhabri, "High performance surface plasmon sensors: Simulations and measurements," *J. Appl. Phys.*, vol. 118, no. 9, Sep. 2015, Art. no. 093105.
[13] F.-C. Chien and S.-J. Chen, "A sensitivity comparison of optical biosensors based on four different surface plasmon resonance modes," *Biosensors Bioelectron.*, vol. 20, no. 3, pp. 633–642, Oct. 2004.
[14] X. Ma, X. Xu, Z. Zheng, K. Wang, Y. Su, J. Fan, R. Zhang, L. Song, Z. Wang, and J. Zhu, "Dynamically modulated intensity interrogation scheme using waveguide coupled surface plasmon resonance sensors," *Sens. Actuators A, Phys.*, vol. 157, no. 1, pp. 9–14, Jan. 2010.
[15] S. Toyama, N. Doumae, A. Shoji, and Y. Ikariyama, "Design and fabrication of a waveguide-coupled prism device for surface plasmon resonance sensor," *Sens. Actuators B, Chem.*, vol. 65, nos. 1–3, pp. 32–34, Jun. 2000.
[16] L. Song, Z. Y. Wang, D. S. Zhou, A. Nand, S. P. Li, B. H. Guo, Y. M. Wang, Z.Q. Cheng, W. F. Zhou, Z. Zheng, and J. S. Zhu, "Waveguide coupled surface plasmon resonance imaging measurement and high-throughput analysis of bio-interaction," *Sens. Actuators B, Chem.*, vol. 181, pp. 652–660, May 2013.
[17] C. Du, L. Liu, L. Zhang, J. Guo, J. Guo, and H. Ma, "Multi-channel hyperspectral fluorescence detection excited by coupled plasmon-waveguide resonance," *Sensors*, vol. 13, no. 10, pp. 13892–13902, Oct. 2013.
[18] K. Liu, M. Xue, J. Jiang, T. Wang, P. Chang, and T. Liu, "Theoretical modeling of a coupled plasmon waveguide resonance sensor based on multimode optical fiber," *Opt. Commun.*, vol. 410, no. 1, pp. 552–558, Mar. 2018.
[19] A. K. Sharma, Rajan, and B. D. Gupta, "Influence of dopants on the performance of a fiber optic surface plasmon resonance sensor," *Opt. Commun.*, vol. 274, no. 2, pp. 320–326, Jun. 2007.
[20] C. Rizal, V. Belotelov, D. Ignatyeva, A. K. Zvezdin, and S. Pisana, "Surface plasmon resonance (SPR) to magneto-optic SPR," *Condens. Matter*, vol. 4, no. 2, p. 50, May 2019.
[21] C. Rizal, S. Pisana, and I. Hrvoic, "Improved magneto-optic surface plasmon resonance biosensors," *MDPI Biomed. Photon. Adv.*, vol. 5, no. 3, p. 15, Jun. 2018.
[22] X. Jiang and Q. Wang, "Refractive index sensitivity enhancement of optical fiber SPR sensor utilizing layer of MWCNT/PtNPs composite," *Opt. Fiber Technol.*, vol. 51, pp. 118–124, Sep. 2019.
[23] J. Ma, Y. Cao, K. Liu, X. Huang, J. Jiang, T. Wang, M. Xue, P. Chang, and T. Liu, "A simple demodulation algorithm for optical SPR sensor based on all-phase low-pass filters," *Proc. SPIE*, vol. 10618, Jan. 2018, Art. no. 106180N.
[24] J. Li and Y. Wang, "Surface plasmon enhanced fiber sensor," *Nanosci. Nanotech. Lett.*, vol. 11, no. 8, pp. 1125–1130, Aug. 2019.

JINYING MA received the B.Eng. degree in optoelectronics information engineering from Tianjin University, China, in 2006, where she is currently pursuing the Ph.D. degree. Her research interest is fiber SPR sensing technology.

KUN LIU received the B.Eng. degree in optoelectronics information engineering and the M.Eng. and Ph.D. degrees in optical engineering from Tianjin University, Tianjin, China, in 2004, 2006, and 2009, respectively. From 2009 to 2010, he worked as a Postdoctoral Researcher with Tianjin University, where he is currently a Professor with the College of Precision Instruments and Optoelectronic Engineering. His research interest includes the development of physics and chemistry sensing systems based on optical fiber lasers.

JUNFENG JIANG received the B.S. degree from the Southwest Institute of Technology, Mianyang, China, in 1998, and the M.S. and Ph.D. degrees from Tianjin University, Tianjin, China, in 2001 and 2004, respectively. He is currently a Professor with Tianjin University. His research interests include fiber sensors and optical communication performance measurement.

TIANHUA XU received the B.Eng., M.Sc., and Ph.D. degrees from Tianjin University, China, in 2005, 2007, and 2011, respectively, and the second Ph.D. degree from KTH Sweden, in 2012. He is currently a Professor with Tianjin University. His research interests include optical communications and fiber sensing.

SHUANG WANG was born in Tianjin, China, in 1982. She received the M.S. degree from the College of Computer Science and Technology, Shandong University, Shandong, China, in 2005, and the Ph.D. degree in optics from Tianjin University, Tianjin, China, in 2014. She is engaged in the research of optical fiber sensing technology, photoelectric detection technology, and other fields.

PENGXIANG CHANG is currently pursuing the Ph.D. degree. His research interest is fiber SPR sensing technology.

ZHAO ZHANG is currently pursuing the Ph.D. degree. His research interest is fiber SPR sensing technology.

JIAHANG ZHANG is currently pursuing the master's degree. Her research interest is fiber SPR sensing technology.

TIEGEN LIU received the B.Eng., M.Eng., and Ph.D. degrees from Tianjin University, China, in 1982, 1987, and 1999, respectively. He is currently a Distinguished Professor with the College of Precision Instruments and Optoelectronic Engineering, Tianjin University. He has published more than 60 articles in scientific and technology journals and proceedings. His research interests include optoelectronics detection and fiber sensing.